Influence of Local Inhomogeneities in the REBCO Layer on the Mechanism of Quench Onset in 2G HTS Tapes

Alexandre Zampa, Sigrid Holleis, Arnaud Badel, Pascal Tixador, Johannes Bernardi, Michael Eisterer

Influence of local inhomogeneities in the REBCO layer on the mechanism of quench onset in 2G HTS tapes

Alexandre Zampa[1], Sigrid Holleis[2], Arnaud Badel[1], Pascal Tixador[1], Johannes Bernardi[3], and Michael Eisterer[2]

[1] University of Grenoble Alpes, CNRS, Grenoble INP, G2ELab – Institut Néel, 38000 Grenoble, FRANCE
[2] TU Wien, Atominstitut, Stadionallee 2, 1020 Vienna, AUSTRIA
[3] TU Wien, USTEM, Wiedner Hauptstraße 8-10, 1040 Vienna, AUSTRIA

***Abstract*—The Resistive-type of Superconducting Fault Current Limiters (R-SFCL) using the second generation of high-temperature superconductors (2G HTS) are well adapted to power grid protection. Almost electrically invisible in normal operation, it quenches and becomes highly resistive in the event of a fault. The tape operation at the transition from the superconducting state to the resistive state is the basis of a R-SFCL. In this scope, we studied the onset of a quench occurring in 2G HTS tapes using high-speed imaging to record the bubble generation in liquid nitrogen. In the first milliseconds of operation, the bubble generation appears highly inhomogeneous. Dissipation is initiated on multiple spots over the tape surface which first expands in the direction of the width of the tape and then along its length. A detailed analysis of the REBCO layer is performed by means of Scanning Hall Probe Microscopy (SHPM) after the optical study of the tapes is completed. Analysis of the local current density distribution demonstrates that the bubble generation occurs at positions of local inhomogeneities in the REBCO layer. These inhomogeneities, well recognized through SHPM, are not reliably described by the critical current as a function of the position derived magnetically (e.g. by traditional TapeStar® measurements). Similar results were obtained on samples from Superpower and SuperOx.**

***Index Terms*—2G HTS tape, R-SFCL, SHPM, propagation**

I. INTRODUCTION

The 2nd Generation of High Temperature Superconductors (2G HTS) are well adapted for the Resistive-type Superconducting Fault Current Limiter (R-SFCL) due to their high linear resistance, high current density and the possibility to operate in liquid nitrogen with low cryogenic costs. This technology relies on the intrinsic transition from the superconducting state to the normal state, also called quench, in the event of a fault in a power grid. The sudden appearance of this resistance limits the current values.

The technology came out of the laboratories with only a few devices installed in power grids. The main barrier to the development of the R-SFCL is the high-cost of the conductor [1]. The development of a cost-effective conductor is an active research interest as demonstrated in the recent European project FASTGRID [2], [3]. There is still no complete understanding of the operation of the 2G HTS tape during such an event while it is known that the quench can be a critical operation phase which can cause degradations [4]. We experimentally observed degradation of the performances of some tapes after successive quenches while the samples were theoretically operating thermally and mechanically in safe conditions.

One way to study the tape operation in fault conditions, i.e. during a quench, is the observation of the bubble generation on the surface of a sample immersed in liquid nitrogen using a high-speed imaging system. This method was adopted in [5] where it was shown that the bubble generation is located along multiple columns, fully developed in the entire width, along the length of the sample. These dissipation columns tend to expand to cover the whole sample length. Other ways exist to study the longitudinal propagation of the dissipation along the length of the tape. The use of fluorescent paint [6] enables the observation of the temperature elevation on the tape or electrical measurements through voltage taps positioned on the tape surface help to measure the Normal Zone Velocity Propagation (NZVP) [7] of these dissipation columns.

However, the dissipation mechanism leading to the formation of these dissipation columns is not fully known. It was assumed in [8] that the quench starts initially at a point and develops transversally to the current path. In this paper, we particularly address the evolution of the dissipation during the onset of a quench on commercial 2G HTS tapes. A high-speed imaging set-up similar to the system in [5] is used with a camera showing a higher resolution and speed. One sample from Superpower and one sample from SuperOx are studied under grid conditions (with a constant voltage). In addition, magnetic analysis of the samples is performed by means of Scanning Hall Probe Microscopy (SHPM). SHPM has proven to be a powerful tool for investigations of the local current distribution in granular superconductors [8]. We associate the local currents

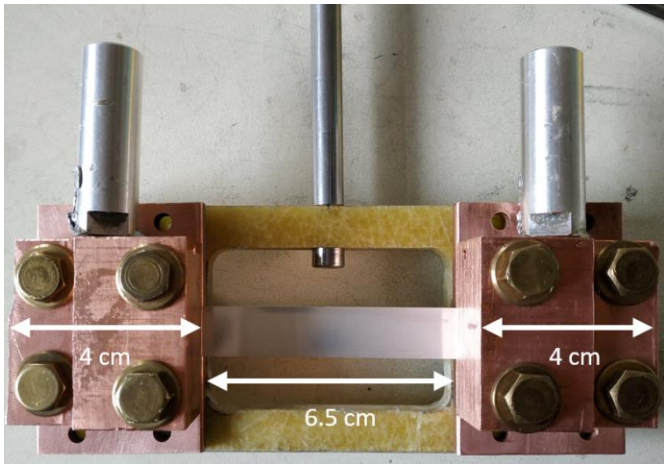

Fig 1. Sample holder used to record the bubble generation on the surface of the tape. The sample is connected to the electrical circuit with pressed contacts.

with the microstructure of the REBCO layer and study the correlation to the initial inhomogeneous dissipation behavior.

II. Experimental Details

The boiling heat transfer regime on the surface of 2G HTS tapes is recorded with a high-speed camera. The samples are placed in R-SFCL conditions during a fault, i.e. they are connected to an electrical circuit with a constant voltage implying a current large enough to initiate thermal runaways. After experiencing one quench, the samples are analyzed through SHPM.

A. Samples

One sample from Superpower and one sample from SuperOx with similar properties are studied. Both tapes have a substrate thickness of 100 µm, a total silver layer thickness of 3-4 µm and similar average critical currents (Ic~500 A/cm$_w$). These two companies use different manufacturing processes to produce their tapes. As an example, the HTS layer growth is done by Metal Organic Chemical Vapor Deposition (MOCVD) with Superpower [9] and by Pulsed Laser Deposition (PLD) with SuperOx [10].

To easily inject the current in these samples, the sample-holder shown in Fig. 1 is used. The sample is connected to the rest of the electrical circuit with pressed contacts and the screws are tightened until the torque equals to 5 Nm. The length of the sample not covered by the current leads is 68 mm for the Superpower sample and 65 mm for the SuperOx sample. The length of the sample is smaller than the full length of tape in a R-SFCL or a superconducting magnet but it is considered to be sufficiently long not to show the influence of the current leads. The structure is mechanically supported by a piece made of fiberglass to ensure no electrical contact between the two current leads except through the sample itself.

The voltage over the sample is measured by one voltage tap connected to each current lead. A 1000 A Fluke rated sensor is used to measure the current through the sample.

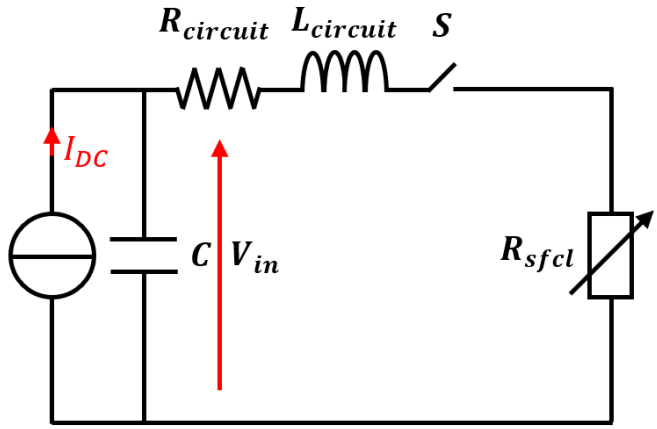

Fig 2. Scheme of the electrical circuit used to initiate thermal runaways in REBCO tape samples.

The sample is immersed in liquid nitrogen in a transparent cryostat at ambient pressure. The direction of its width is colinear with the vertical direction.

B. Fault current set-up

The fault current set-up aims to initiate thermal runaways in the samples. To do so, the current leads of the sample holder are connected to the DC circuit displayed in Fig.2. It consists of a voltage source realized with a supercapacitor (165 F-48 V) fed by a constant DC current source, whose capacity is big enough to ensure a negligible voltage drop during the pulse. The input voltage is V_{in}=18 V and the equivalent impedances of the circuit are $R_{circuit}$ equals to 21 mΩ and $L_{circuit}$ to 6 µH. The absence of zero-crossing in DC mode makes the fast current interruption more difficult. To achieve it, the switch S is composed of five half-bridge MOSFETs in parallel. The user controls the closing of S through a function generator delivering a single pulse with a duration Δt of 10 ms to the MOSFET.

C. High-speed imaging

A Phantom V311 high-speed camera is positioned facing the surface of the 2G HTS sample on the superconducting side. Its exposure time is set to 3 µs and its frame rate to 50000 fps, which means that an image is recorded every 20 µs to observe phenomena with high dynamics. The resolution is 560x96 pixels. A powerful light source is used to work with a small exposure time.

To make synchronous recordings of the electrical measurements by the scope and the images by the high-speed camera, the raising edge of the pulse controlling the closure of S triggers these two devices simultaneously.

D. Scanning Hall Probe Microscopy

Remnant field profiles at 77 K of both samples were obtained by means of SHPM. For these experiments, the tape is immersed in a liquid nitrogen bath where the magnetization of the sample is induced by a permanent magnet which is dragged along the length of the tape just above the surface. A Hall probe

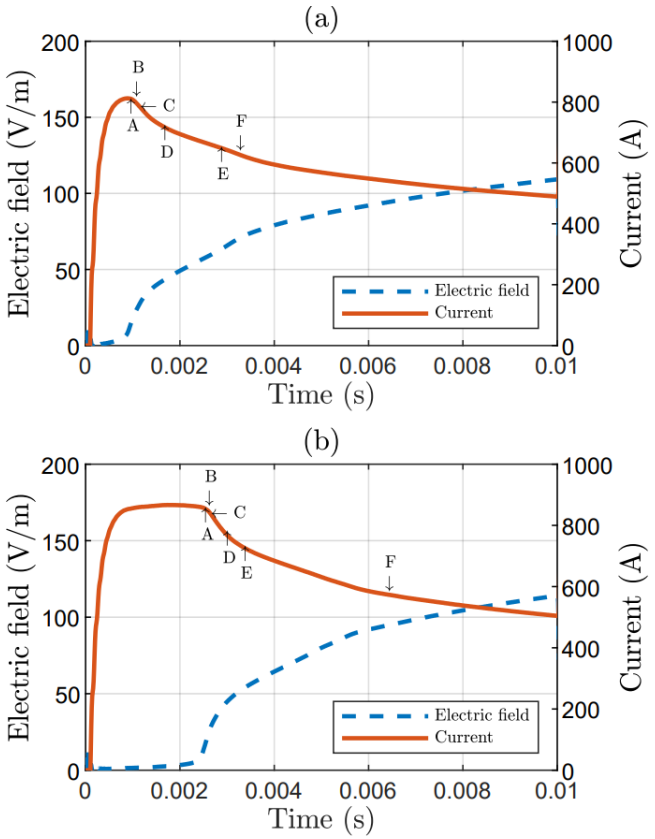

Fig 3. Electric field (dashed blue line) and current (solid red line) as a function of the time measured on the (a) Superpower sample and (b) SuperOx sample. The letters refer to the pictures given in Fig. 4.

with an active area of 50 x 50 μm^2 is mounted at the end of a cantilever. Contact to the sample surface is monitored by strain gauges. The distance from the Hall probe to the sample surface is set to about 30 μm to achieve high resolution scans. A more detailed description of the setup can be in found in [11].

The local distributions of the critical current density $J_c = \sqrt{J_x^2 + J_y^2}$ as well as the longitudinal (J_x) and transverse (J_y) current densities are obtained from the trapped field profiles by an inversion of Biot-Savart's law [12].

The critical current, I_c, is obtained by summing up all currents flowing in the discrete elements between two measurement points along y: $I_c(x) = \sum J_x d\Delta y$, where d and Δy denote the thickness of the superconducting layer and the distance between two points of the measurement grid, respectively. The summation is performed over all elements of each row in the J_x-matrix.

III. Results and Discussion

A. Bubble generation

Fig. 3 shows the current in the circuit and the electric field (voltage over the sample divided by its length) across the (a) Superpower sample and the (b) SuperOx sample.

The images of the Superpower sample recorded during the test are displayed in Fig. 4 (a). The first bubble generation spot appears at 0.88 ms in image A. Additional spots are observed in images B and C. The bubble generation starts locally on the edges of the sample. At 2.80 ms, all the spots have expanded and cover the entire width where they were initially appearing to form dissipation columns. These columns propagate then in the longitudinal direction of the sample until the whole sample is bubbling at 5.20 ms.

Fig. 4 (b) shows the images at several times of the SuperOx sample. The two first bubble generation spots appear at 2.46 ms. Additional dissipation spots are present at 2.54 ms and 2.66 ms. Images B and C highlight that bubbles locally appear at the center of the width of the sample. In a similar way to what has been observed on the Superpower sample, the spots expand first in the direction of the width of the tape to form dissipation columns (all existing at 3.30 ms) and then enlarge in the longitudinal direction of the sample until dissipation covers the entire sample at 6.36 ms. The evolution of the dissipation over these samples is similar to what was predicted in [8]. During the first milliseconds of the test where a quench is initiated on both Superpower and SuperOx samples, the heat dissipation through boiling heat transfer is inhomogeneous. The current initiates bubble generation on local spots over the tape surface, located on the center of the width on the SuperOx sample and on the edges on the Superpower sample. The dissipation propagation occurs in two directions: first, rapidly in the order of tens of meters per second along the width to form dissipation columns and then, slower depending on the instantaneous current, along the length until the bubbles cover the whole surface.

The critical current as a function of the position, generally measured in self-field at 77 K with a characterization machine such as Tapestar® [13], gives the distribution of the superconducting properties along the tape length. One assumption explaining that the bubble generation appears on distinct and localized positions at the onset of a quench would be a lower critical current at these positions and a higher critical current elsewhere. In order to confirm this hypothesis, the HTS layer is analyzed using SHPM.

B. Local current flow

While the quench experiments were conducted with high currents in a fast and dissipative regime, the SHPM measurements were conducted under quite different conditions. Here, the superconductor is in the remnant state where closed loops of nearly loss-free currents flow around the superconducting area and have to meander around non-superconducting areas in the remnant state.

The first panel in Fig. 5 (a) shows the measured trapped field of the Superpower tape at 77 K with a spatial resolution of 150 μm. The maximum remnant field is about 33 mT and some elongated inhomogeneities can be observed in the field profile along the edges of the tape as well as in the center. When overlaying the remnant field scan with image E in Fig. 4 it becomes evident that the positions of the bubbles are in perfect agreement with the elongated inhomogeneities, as can be seen

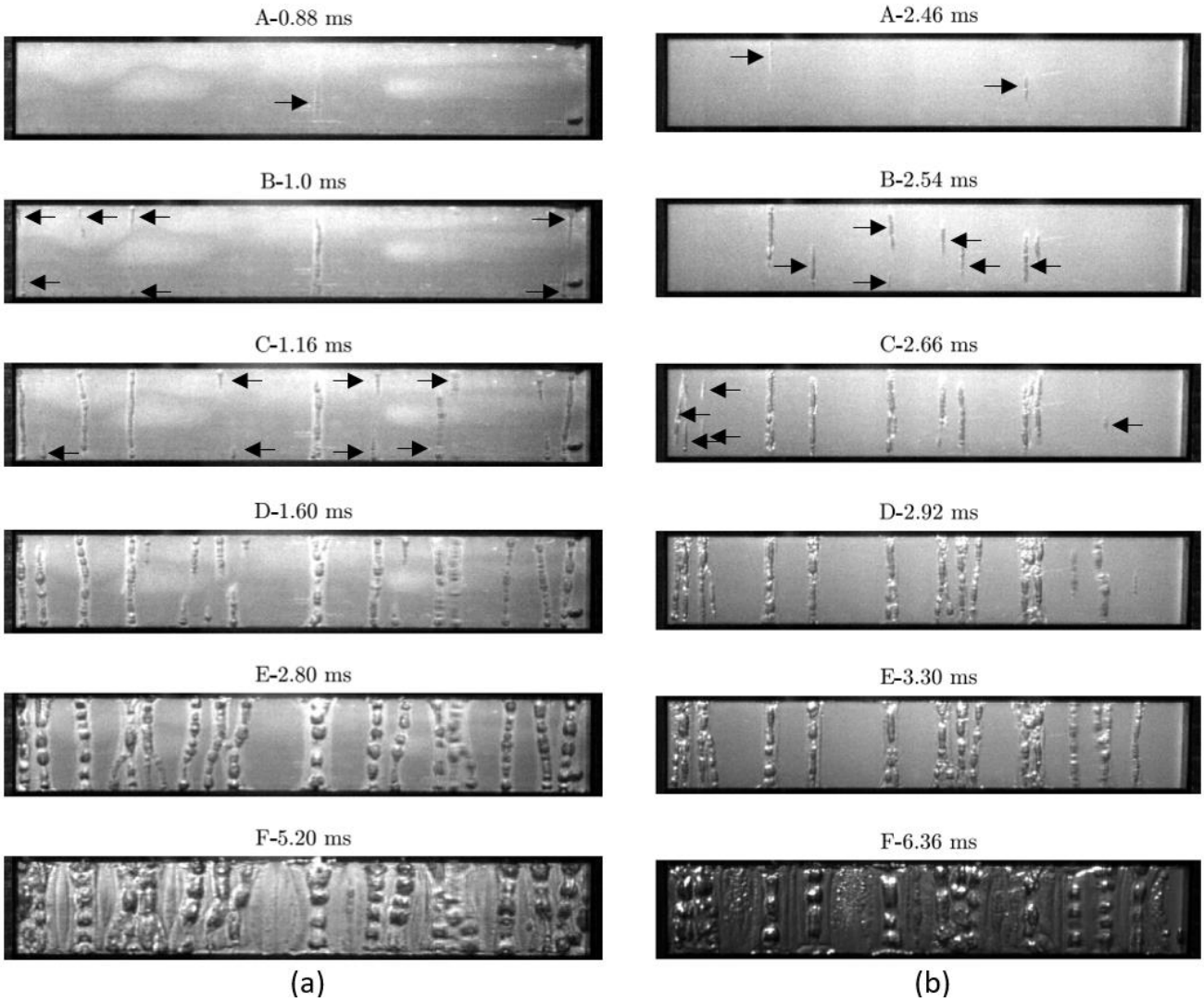

Fig. 4. Images of (a) the Superpower sample and (b) SuperOx sample at several times during the tests. Starting points of bubbles are indicated by black arrows.

in the second panel in Fig. 5 (a). The third panel illustrates the calculated J_c distribution. Low J_c values in the center and on the corners result from geometrical constraints where the currents change direction. From the J_x matrix, it is possible to calculate the local I_c along the length of the tape, see Fig. 6 (a). The blue line shows the average I_c corresponding to the position of the underlying tape image. A clear drop in I_c can be observed in the center of the tape where the first bubbles start, however, the I_c at this position is only 2.5% lower than the maximum I_c observed in this tape. At some other bubble positions along the tape no significant drop in I_c is observed.

A much more powerful tool to visualize inhomogeneities in the local current distribution resulting from defects are the transverse current densities J_y. Using the J_y matrix we define the meandering currents $I_y(x) = \frac{1}{N}\sum|J_y|d\Delta x$, with N being the number of elements along the sample width. Fig. 6 (b) shows the meandering currents (blue line) on top of the tape image. The double peaks at the positions of the dissipation columns indicate high J_y values somewhere along the width of the tape at these positions. By comparing the J_y map to the remnant field profile it becomes clear, that at each elongated inhomogeneity there are two high J_y areas in the upward and downward direction, i.e. the currents have to bypass a defect in the superconducting layer, as can be seen in the lower two panels of Fig. 5 (a). Such areas are very prominent at the upper and lower edge of the Superpower tape. When overlaying the J_y map with image C in Fig 4., it is evident that the bubbles first originate in areas with high J_y values, indicated by the black arrows in the lowest panel in Fig. 5 (a).

The local current investigations on the SuperOx tape are shown in Fig. 5 (b). The overall remnant field profile appears more homogeneous, the maximum trapped field is about 44 mT and there are much less elongated inhomogeneities along the edges of the tape. The second panel shows the overlay of image E in Fig 4. and the trapped field profile. Again, the positions of the bubbles are in perfect agreement with the magnetic profile. The J_y maps in the lower two panels show fewer areas with high values at the edges, but in cases where there are high J_y values,

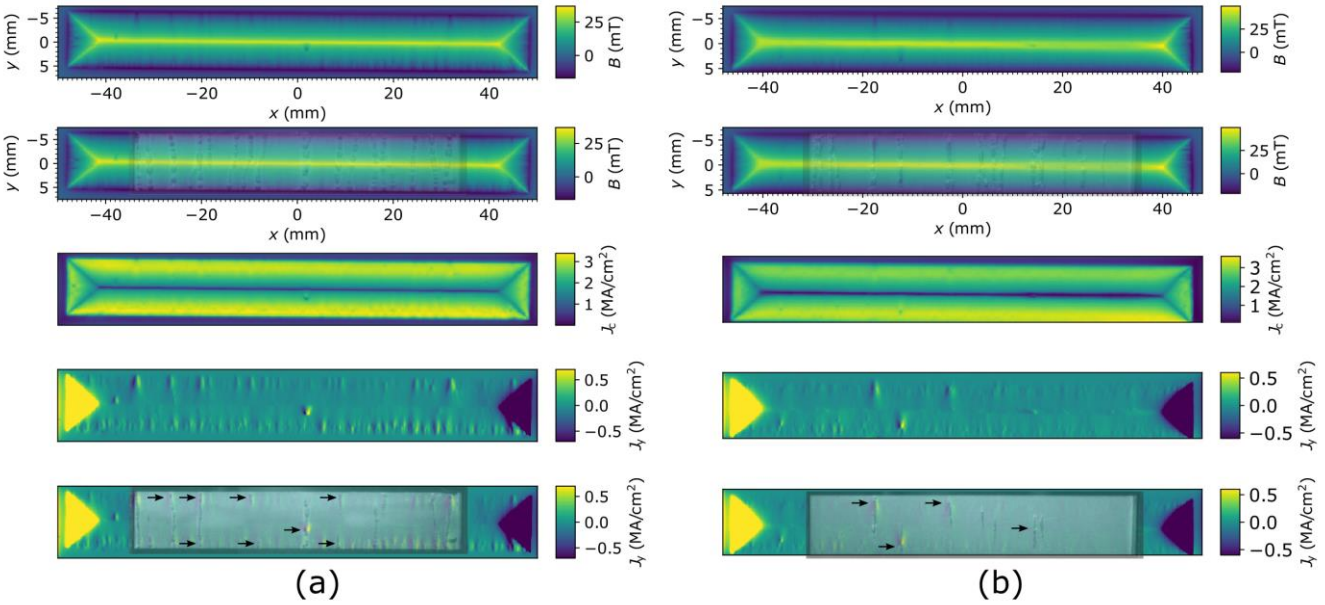

Fig. 5. Measured remnant field profiles and calculated current density maps of the Superpower tape (a) and SuperOx tape (b). The two upper panels show the remnant field profiles measured with a spatial resolution of 150 µm without and with overlay of the corresponding bubble image. The middle panel shows the calculated J_c map of both tapes. The two lower panels visualize the current densities in y-direction. At points where bubbles start to emerge (indicted by black arrows in the overlaid image) J_y shows high values in the upward and downward direction.

they agree well with starting points of bubbles, as indicated by the black arrows in the lowest panel in Fig. 5 (b).

These results show that the positions of bubble generation columns match the positions of inhomogeneities, recognized by high J_y areas. Monitoring the critical current I_c alone is not sufficient to describe the onset of a quench in 2G HTS tapes. The visualization of the bubble generation over the surface of a tape enables the recognition of inhomogeneities. However, from these observations it is not possible to determine if the dissipation is initiated at the exact position of the defect or its direct surrounding.

C. Defects in the REBCO layer

In order to investigate the origin of the bubbles further, the silver coating of both tapes was removed by chemically etching with hydrogen peroxide, ammonium hydroxide and distilled water in a ratio 1:1:1. A small piece from the center of the Superpower tape was cut out in order to obtain a sample where one line of bubbles starts in the middle and one at the edge of the tape. The right panel in Fig. 7 shows the trapped field profile of this center piece at 77 K with a spatial resolution of 50 µm. By comparison with the trapped field scan of the entire tape, areas *a* and *b* were identified as starting points of bubbles. The left panel in Fig. 7 shows the high-speed imaging photos where the bubbles in area *a* and *b* start at 0.56 ms in the center and at 0.7 ms at the edge, respectively.

Scanning Electron Microscopy (SEM) images were obtained with a FEI Quanta 250 FEGSEM with an accelerating voltage of 20 kV. The upper panel in Fig. 8. shows an SEM image of area *a* from Fig. 7. While the surrounding area shows the typical smooth surface morphology of a YBCO film with some misoriented grains, in the center of the image a large area of randomly oriented grains that appear brighter in the secondary electron detector can be observed. It can be assumed that a scratch in the substrate or buffer layers hindered the epitaxial growth of the superconducting layer in this area. A similar defect was found in area *b* of the Superpower tape (lower panel of Fig. 8.). EDX analysis (not shown here) showed no difference in the spectrum of the smooth and granular film surface, therefore secondary phase precipitates can be excluded as the cause of the bubble origin. Along the edges of the Superpower tape many such areas were found, and also in places where bubbles start in the SuperOx tape. From these comparisons it is evident, that an area of just a few microns of non-epitaxial film growth can be the origin of inhomogeneous quench behavior.

These small areas of tiny misoriented grains are the reason for thermal instabilities of the tape despite their rather small influence on the critical current itself. At negligible dissipation, the current flows around such defects and transverse currents can be deduced from the magnetic field profile (Fig. 5). The bubble formation on the other hand starts at a much higher dissipation level, the mean electric field already being a few volts per meter. Since the electric field is primarily oriented along the tape in the latter case, meandering is reduced compared to the low dissipation regime and significant currents can be expected also in disturbed areas. An intermediate loss regime was established during scanning laser spectroscopy, where a closed correlation between the microstructure, meandering currents and local losses were found, too [14]. The

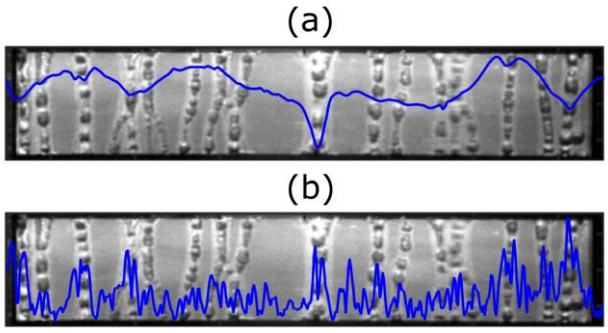

Fig 6. (a) Average I_c of the Superpower tape calculated from the measured remnant field (blue line). A clear kink is visible in the middle where the first bubbles appear. The I_c at this position is only 2.5% lower than the maximum. (b) The meandering currents I_y show clear increases at the positions of the dissipation columns.

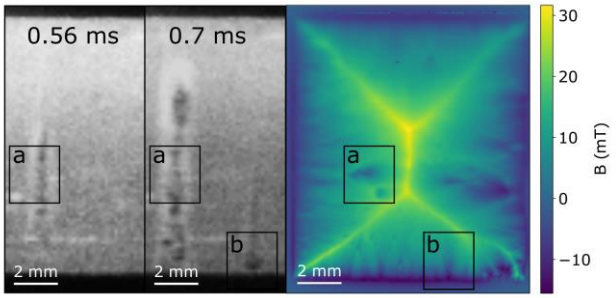

Fig 7. Remnant field scan of the middle section of the Superpower tape with a spatial resolution of 50 µm (right panel) and corresponding images of the bubble formation (left panel). Areas *a* and *b* indicate the starting points of bubbles at 0.56 ms and 0.7 ms, respectively.

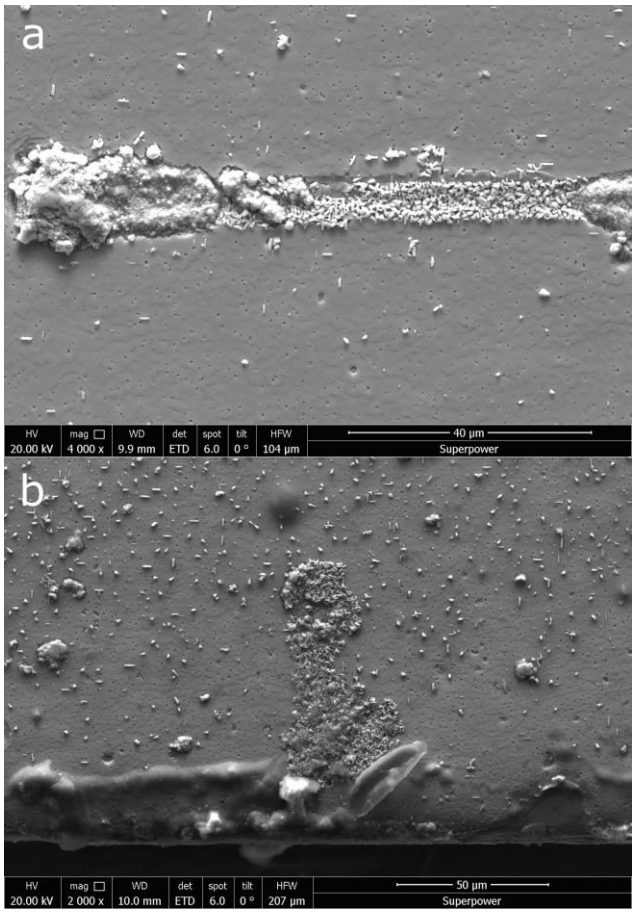

Fig. 8. SEM images of areas *a* and *b* in Fig. 7. The images show defects in the REBCO layer. The granular nature of these defects indicates a non-epitaxial growth of the superconducting film.

first bubbles occur at or very close to an area of misoriented grains. Both, the local current density and electric field have to be high at this first hot spot, since the power density is given by their product. The electric field has to be very inhomogeneous since only small areas quench at the beginning, where the local electric field is much higher than the mean one. The resulting heating reduces the local critical current density pushing the currents on the remaining width of the tape which leads to enhanced dissipation there and consequently to the formation of a column of bubbles. The propagation of these columns on the longitudinal direction of the tape increases the mean electric field whereas the current decreases. At the end, the local and mean electric fields are similar, therefore, bubble generation occurs nearly homogeneously over the surface.

IV. Conclusion

This paper presents an in-depth observation of the onset of a quench in 2G HTS tapes using an optical study associated with the local current distribution obtained by SHPM. During the quench onset, the bubble generation appears localized on distinct spots over the tape surface. These spots tend to appear on the edges on the Superpower sample and on the center of the width on SuperOx sample. They first expand rapidly in the direction of the width of the sample to form columns of dissipation. These columns then propagate slower, depending on the instantaneous current, in the longitudinal direction of the sample until the boiling covers the whole tape.

The analysis of the REBCO layer with SHPM demonstrates that the origin of bubbles, recorded by the high-speed camera, are local inhomogeneities in the tape. These inhomogeneities cause current meandering at very low electric fields and dissipation at overcurrents. The critical current as a function of the position alone, measured by SHPM or the traditional TapeStar®, is less sensitive to small inhomogeneities and not sufficient to describe the local dissipation phenomena. This can be seen in the transverse current density which proves to be more suitable to describe the very beginning of a quench in a 2G HTS tape. Comparison to the microstructure of the superconducting layer reveals that the inhomogeneous current flow is caused by areas of non-epitaxial film growth. These areas are responsible for hot spot formation at large overcurrents.

With the present results, it is not possible to conclude about the initial position of the dissipation which can be either on the defect or in its direct surrounding. Modelling efforts will be carried out to answer this open question.

ACKNOWLEDGMENT

This research was funded in part by the Austrian Science Fund (FWF): I 4146-N36.

Thank you to M.Gibert & J.Vessaire for the kind help with the camera and to A. Derbey & B. Sarrazin for the development of the DC switch.

REFERENCES

[1] A. Safaei, M. Zolfaghari, M. Gilvanejad, and G. B. Gharehpetian, ‘A survey on fault current limiters: Development and technical aspects’, *International Journal of Electrical Power & Energy Systems*, vol. 118, p. 105729, Jun. 2020, doi: 10.1016/j.ijepes.2019.105729.

[2] P. Tixador *et al.*, ‘Status of the European Union Project FASTGRID’, *IEEE Trans. Appl. Supercond*, vol. 29, no. 5, pp. 1–5, Aug. 2019, doi: 10.1109/TASC.2019.2908586.

[3] Fastgrid Consortium. "Cost effective FCL using advanced superconducting tapes for future HVDC grids" https://www.fastgrid-h2020.eu (accessed Jan. 18, 2022).

[4] H. Song, F. Hunte, and J. Schwartz, ‘On the role of pre-existing defects and magnetic flux avalanches in the degradation of YBa2Cu3O7–x coated conductors by quenching’, *Acta Materialia*, vol. 60, no. 20, pp. 6991–7000, Dec. 2012, doi: 10.1016/j.actamat.2012.09.003.

[5] N. T. Nguyen and P. Tixador, ‘A YBCO-coated conductor for a fault current limiter: architecture influences and optical study’, *Supercond. Sci. Technol.*, vol. 23, no. 2, p. 025008, Feb. 2010, doi: 10.1088/0953-2048/23/2/025008.

[6] R. Gyuráki, F. Sirois, and F. Grilli, ‘High-speed fluorescent thermal imaging of quench propagation in high temperature superconductor tapes’, *Supercond. Sci. Technol.*, vol. 31, no. 3, p. 034003, Jul. 2018, doi: 10.1088/1361-6668/aaa703.

[7] J. Giguère, C. Lacroix, F. Dupuis-Desloges, J.-H. Fournier-Lupien, and F. Sirois, ‘High normal zone propagation velocity in copper-stabilized 2G HTS coated conductors’, *Supercond. Sci. Technol.*, vol. 34, no. 4, p. 045010, Apr. 2021, doi: 10.1088/0953-2048/18/10/018

[8] A. Heinrich, ‘Quenching of superconductivity and propagation of the resulting normal phase in YBCO films’, *Supercond. Sci. Technol.*, vol. 18, no. 10, p. 1354, Aug. 2005, doi: 10.1088/1361-6668/abe4b5.

[9] V. Selvamanickam *et al.*, ‘Recent Progress in Second-Generation HTS Conductor Scale-Up at SuperPower’, *IEEE Trans. Appl. Supercond.*, vol. 17, no. 2, pp. 3231–3234, Jun. 2007, doi: 10.1109/TASC.2007.899360.

[10] S. Lee *et al.*, ‘Development and production of second generation high T_c superconducting tapes at SuperOx and first tests of model cables’, *Supercond. Sci. Technol.*, vol. 27, no. 4, p. 044022, Apr. 2014, doi: 10.1088/0953-2048/27/4/044022.

[11] M. Lao *et al.*, ‘Planar current anisotropy and field dependence of J_c in coated conductors assessed by scanning Hall probe microscopy’, *Supercond. Sci. Technol.*, vol. 30, no. 2, p. 024004, Feb. 2017, doi: 10.1088/1361-6668/30/2/024004.

[12] F. Hengstberger, M. Eisterer, M. Zehetmayer, and H. W. Weber, ‘Assessing the spatial and field dependence of the critical current density in YBCO bulk superconductors by scanning Hall probes’, *Supercond. Sci. Technol.*, vol. 22, no. 2, p. 025011, Feb. 2009, doi: 10.1088/0953-2048/22/2/025011.

[13] S. Furtner, R. Nemetschek, R. Semerad, G. Sigl, and W. Prusseit, ‘Reel-to-reel critical current measurement of coated conductors’, *Supercond. Sci. Technol.*, vol. 17, no. 5, pp. S281–S284, May 2004, doi: 10.1088/0953-2048/17/5/037.

[14] Kiss